OAK RIDGE National Laboratory

Consortium of Advanced Battery Simulation: Development of Computational Framework for Battery Analysis under Extreme Conditions

PI : Srikanth Allu

TEAM : Srdjan Simunovic, Sergiy Kalnaus, Hsin Wang, Gavin Wiggins, Kevin Lai

June 12, 2019

Project ID: bat300

ORNL is managed by UT-Battelle, LLC
for the US Department of Energy

U.S. DEPARTMENT OF ENERGY

Overview

Timeline

- Start
  - October 2015
- Finish
  - September 2019
- Percent complete: 75%

Barriers Addressed

- Performance
- Abuse Tolerance, Reliability, and Ruggedness
- Life

Budget

- FY18
  - Total Funding: 650K
- FY19
  - Total Funding: 850K

Partners

- LBNL
- SNL
- ANL
- as well as the NREL-led CAEBAT project team

Milestones (FY19)

IDs indicate whether milestones are primarily experimental (E), computational (C), or integrated (I).							
ID	FY18	Lead	Q1	Q2	Q3	Q4	Status
C.4	Demonstration of validated constitutive models & failure criteria for electrode materials & spirally wound, wound prismatic, & stacked electrodes under bending for pouch cell	ORNL	P				Completed
C.5	Demonstrate improved computational efficiency on a benchmark pack-level simulation using a hierarchy of electrochemical models for US06 drive cycle	ORNL		P			Completed
C.6	Coupled electrochemical-mechanical simulations of plating conditions during fast charge and overcharge scenarios	ORNL				P	Ongoing
I.6	Deployment of VIBE/OAS with efficient, validated mechanistic models	ORNL				S	Ongoing

Overall project outcome and goals

Expected Outcomes / End-of-project goals	
Experimental protocols	New tests for characterizing deformation and failure modes of Li-ion cells and properties of constituents. Tests will include micro- and nano-indentation to obtain strength and elastic properties of electrode secondary particles and micro-scratch tests to study aggregate strength. The compression and bending tests will be able to freeze the internal cell configuration and characterize its evolution
Data	Property data for mechanical, electrical, and electrochemical models. The data for constitutive properties of electrode bonded aggregates; compressive strength of cathode secondary particles, failure criteria for electrodes and their assemblies; SOC-dependent diffusivities; ionic conductivities of electrodes; cell impedance. Validation data for microstructure-based modeling, details of 3D electrode microstructure, microscopy on cycled/abused electrodes; surface temperatures in a cell during cycling and internal short.
Models	(1) Impedance models for performance under rapid cycling, (2) Efficient hybrid models for pack simulation with large local thermal gradients, (3) Constitutive models for electrode deformation based on composition, (4) Constitutive and failure models for spirally wound, wound prismatic, and stacked electrodes in pouches and hard cases, (5) Microstructure models for coupled thermal-electrochemical-mechanical behavior under normal and abuse conditions, (6) Methods for homogenizing mechanical and transport properties from microstructure to electrodes and cells, (7) Criteria for criticality of internal short-circuits.
Software	VIBE, including OAS and physics components, will be released continuously throughout the project. By the end of project VIBE will include (1) integration of additional external components developed during this period, (2) new components for microstructure modeling, (3) new hybrid/adaptive components for efficient simulation of modules and packs.

Approach - Understanding of Failure Mechanisms

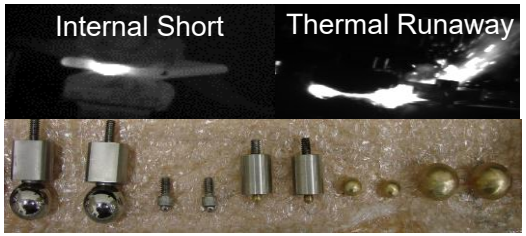

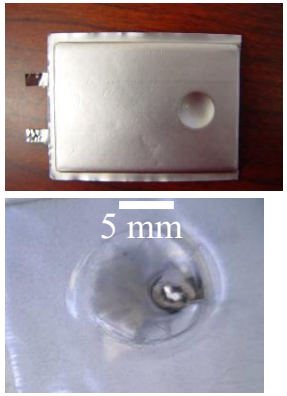

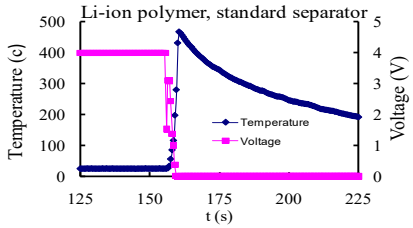

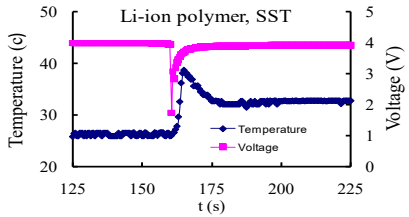

- Observation of Voltage drop -> Electrode-to-Electrode Contact -> Separator Failure
- Open cells (destructive): extensive electrode damage, separator failure – hard to pin-point the failure
- Cross-section imaging: Only see one cross-section, better view of deformation, hard to see separators, damages in cutting and polishing
- 3D X-ray Computed Tomography: XCT – non-destructive, clear view of cathode and copper current collector – identified failure mechanism under compressive load

Technical Accomplishment : XCT Showed Mud-cracks in Copper Current Collector

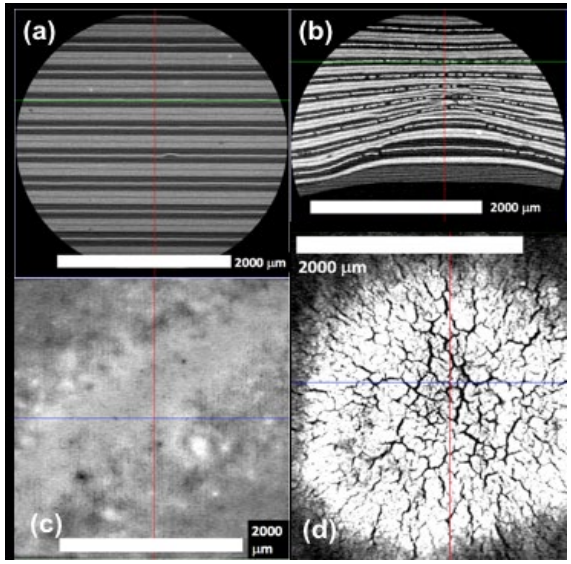

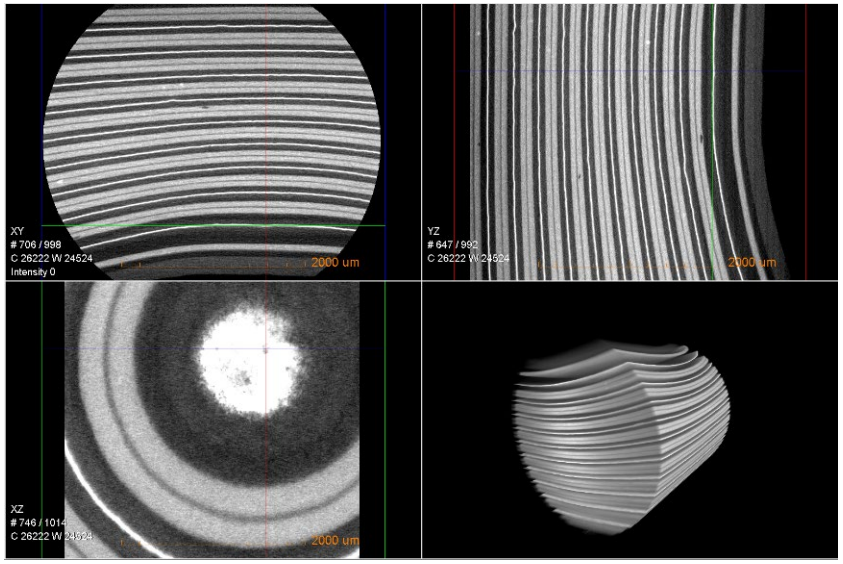

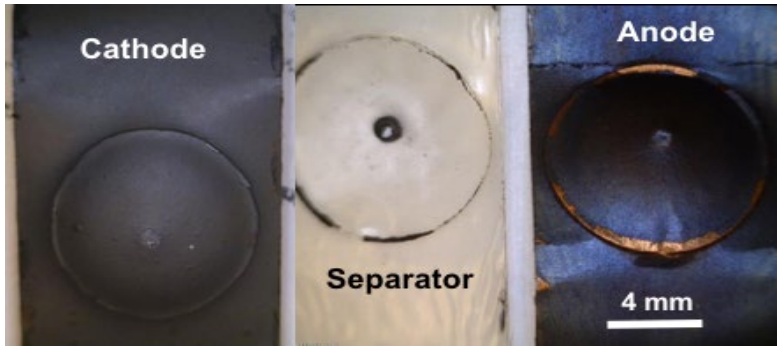

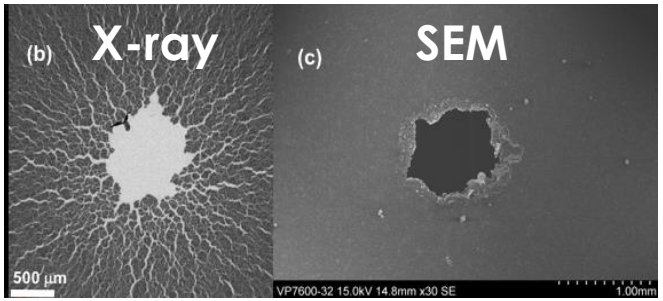

OAK RIDGE National Laboratory

Open slide master to edit

Technical Accomplishment:
SEM Image of Copper Current Collectors

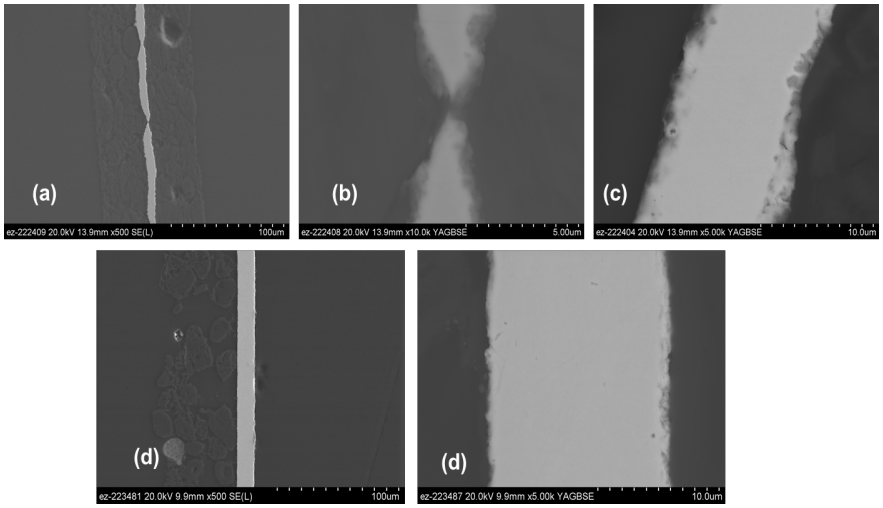

EPMA and STEM Element Maps

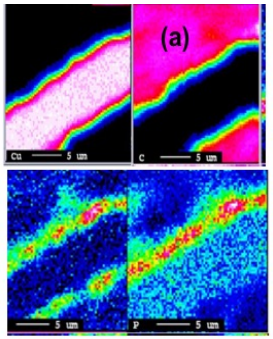

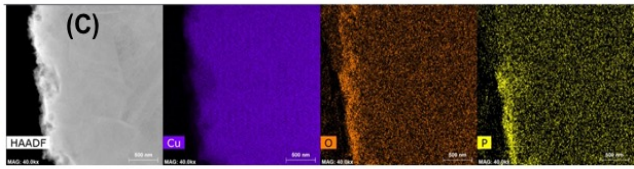

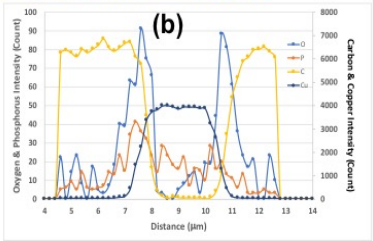

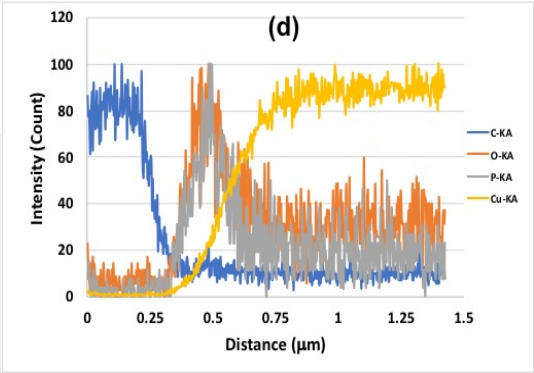

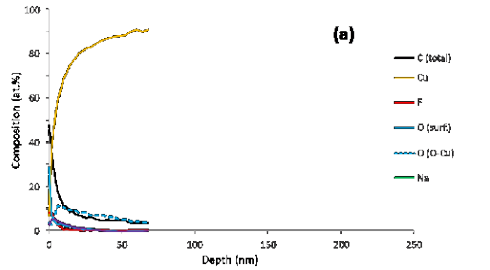

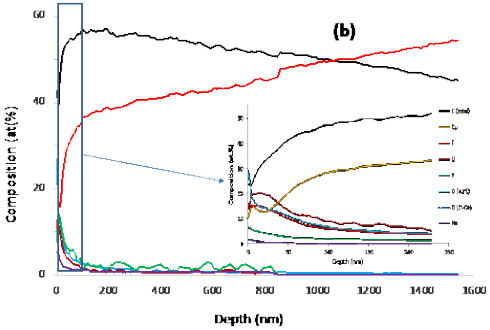

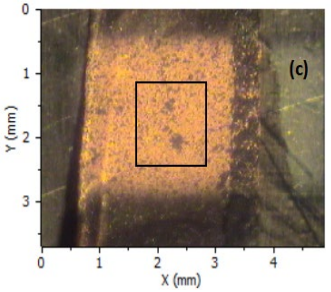

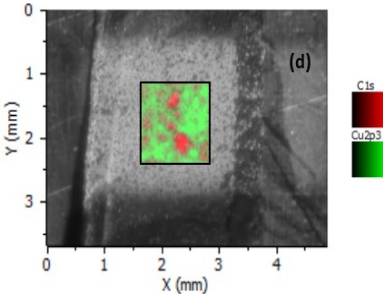

XPS Depth Profiling

OAK RIDGE National Laboratory

Technical Accomplishment: Study on Overcharging: $Li(Ni_{0.6}Co_{0.2}Mn_{0.2})O_2$ (NCM622)

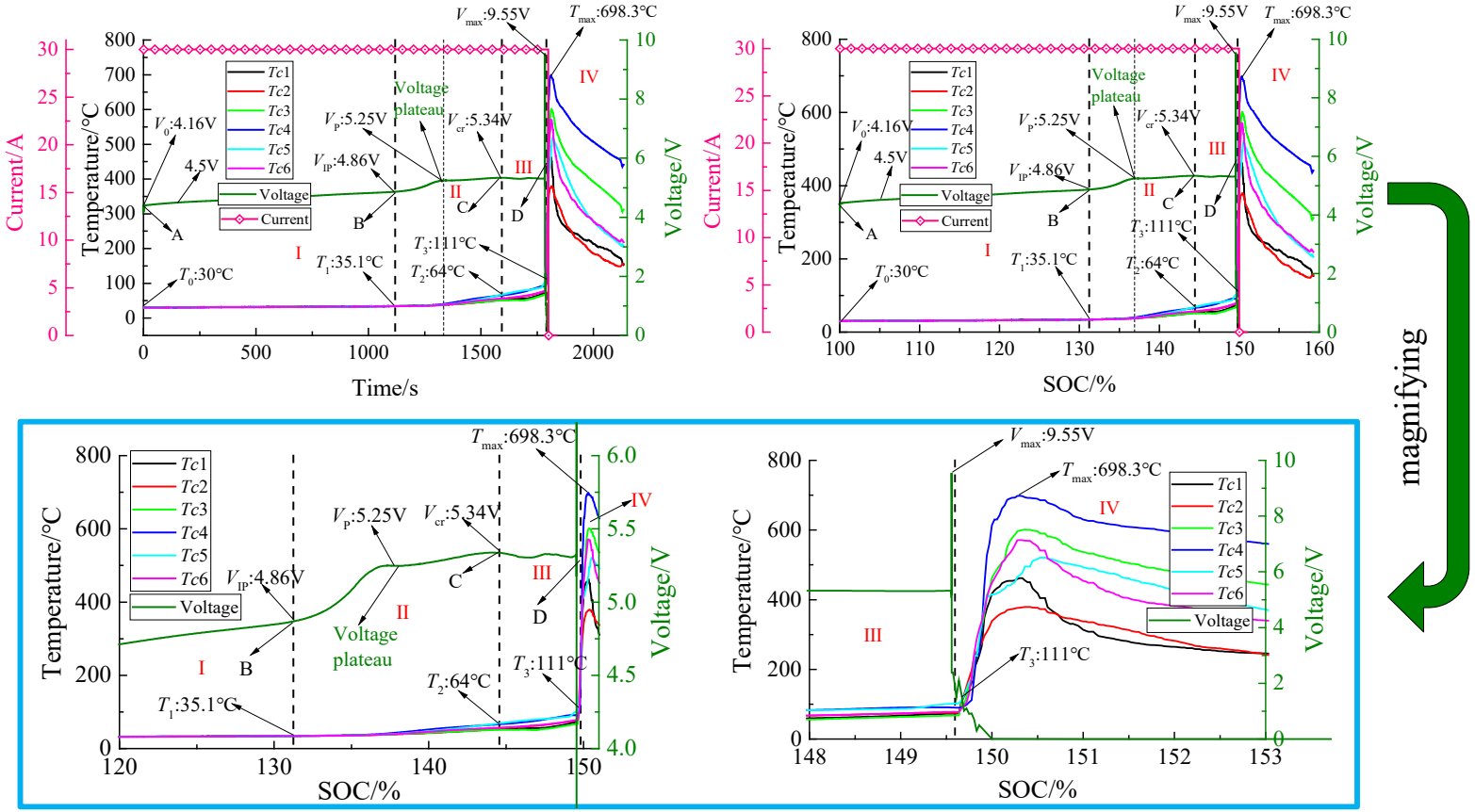

X Zhu, Z Wang, Y Wang, H Wang, C Wang, L Tong, M Yi, "Overcharge investigation of large format lithium-ion pouch cells with Li (Ni0. 6Co0. 2Mn0. 2) O2 cathode for electric vehicles: Thermal runaway features and safety management method", *Energy* 169, pp868-880 (2018)

OAK RIDGE National Laboratory

Approach: Mechanical Model using Microstructure Information

1. Formation of the active material electrode layer during the calendaring process
   - Discrete element method (DEM)
2. The effect of the resulting internal structure on the overall mechanical properties
   - DEM
   - Analysis of the internal rearrangement during the loading
3. Upscaling of the microstructure mechanical model into the effective continuum model
   - Continuum constitutive model homogenization for the representative volume element (RVE)
   - Parameters for the continuum models

Approach : Model Setup

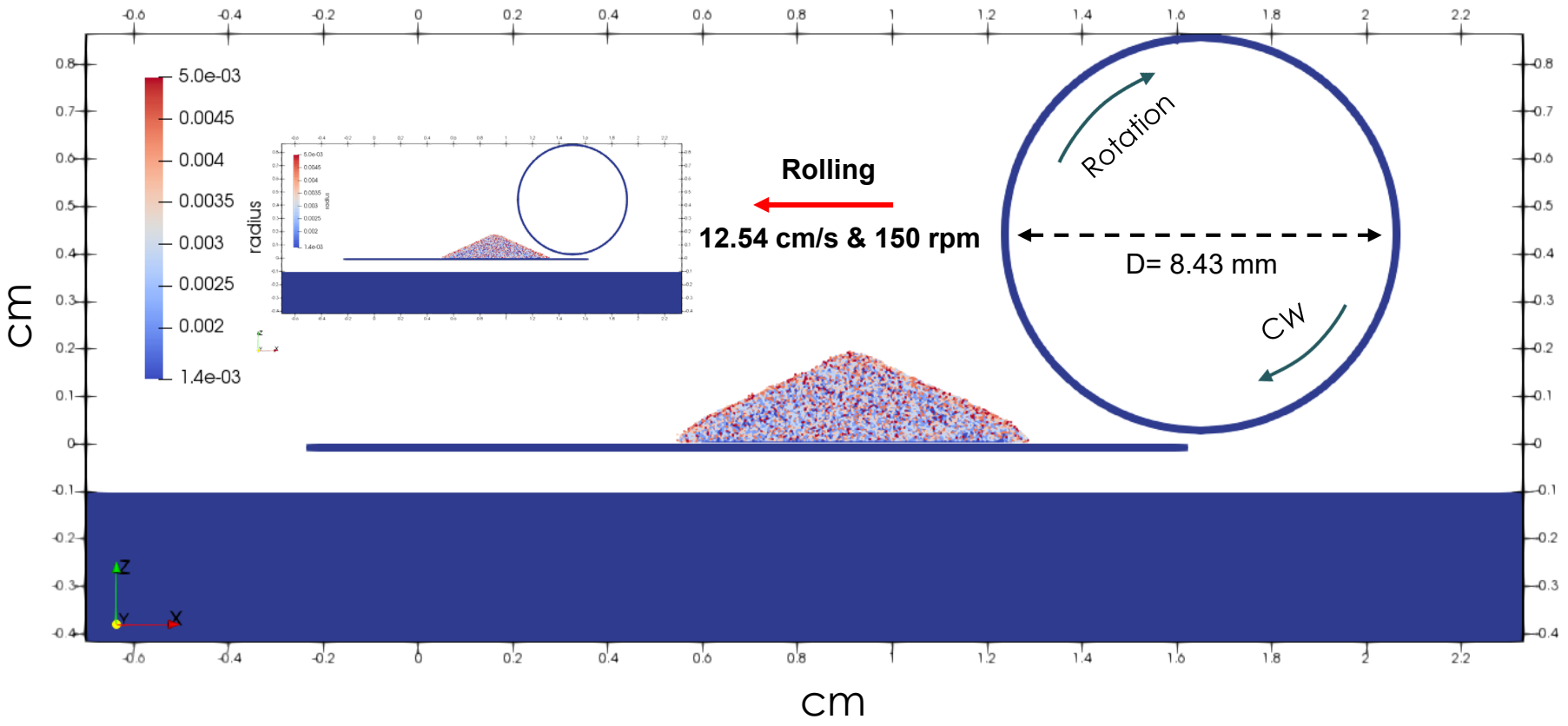

- Gaussian distribution of particle size
- We are currently evaluating different particle parameter interaction models based on material properties from the literature.

Technical Accomplishment: Powder Spreading and Compaction

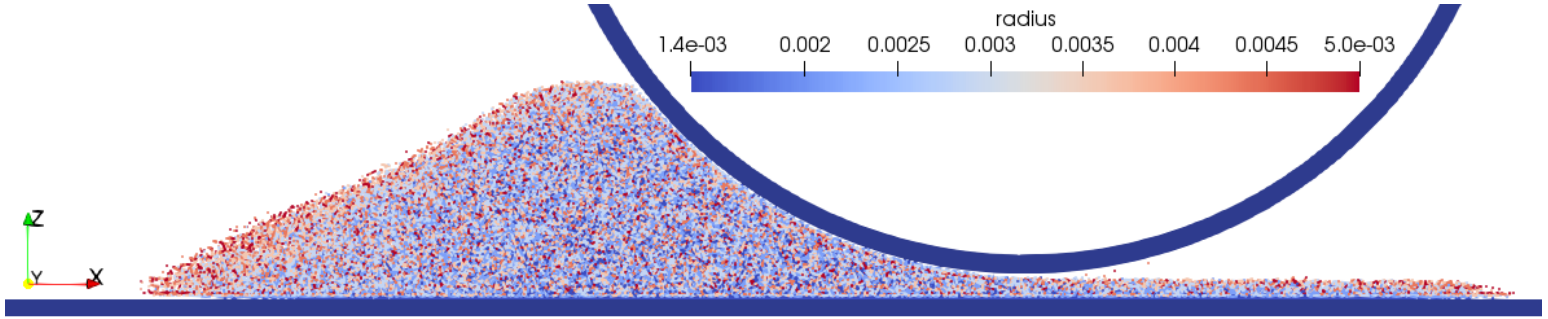

* Particle location

* Particle size

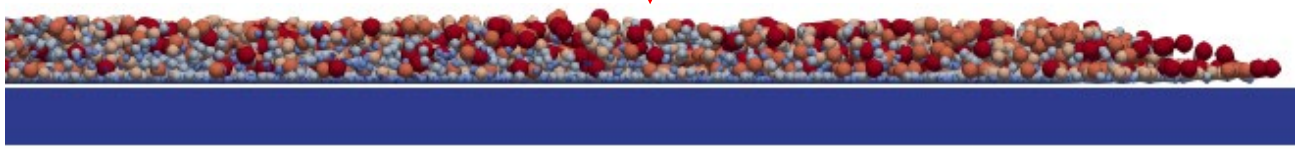

- Roller influences particle distribution through thickness and segregation in the plane.
- Compaction layer is created in the interaction of roller with particles
- Very few experiments are available for validation.

Approach :Microstructure-based Continuum Model

- Active material microstructure and composition determines mechanical stiffness and anisotropy.
- Two stages of influence:
  1. Microstructure and properties that develop due to compaction / calendaring / assembly of cells
  2. Microstructure and property evolution during deformation
- Microstructure of the 1st stage has dominant effect on the effective material properties.
- The microstructural changes in the 2nd stage can be modeled by constitutive model parameters and experiments.

Experimental Data:

- Li $Ni_{1/3}Mn_{1/3}Co_{1/3}O_2$ (NMC)-based cathodes
- Varying weight percent of carbon black and binder (2–5 wt%)
- Applied pressures (0-2000 bar)
- X-Ray tomography of large volumes 700x700x70 microns
- Data is used for particle size distribution, location, shape, etc.
- The data consists of sets of raw, processed and segmented images that give voxelized data.
- Data was used to develop different models and representations of battery microstructure using Fabric Tensor

Approach: Microstructure Model in a Nutshell

- Use length scale of AM particles
- Employ the microstructure metric as a directional measure of microstructure

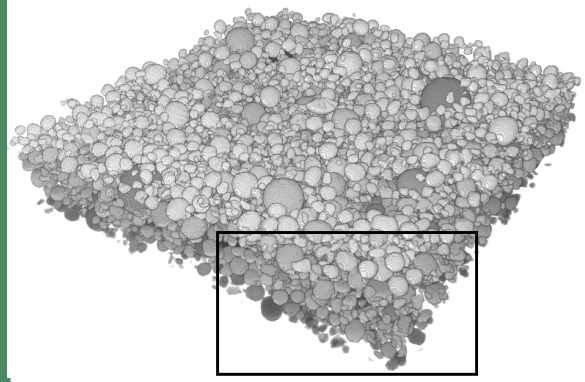

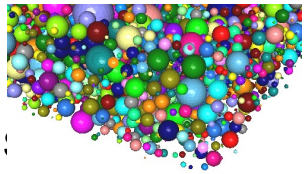

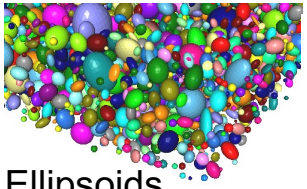

Ellipsoids

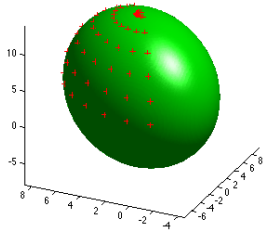

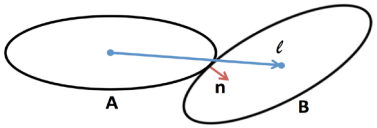

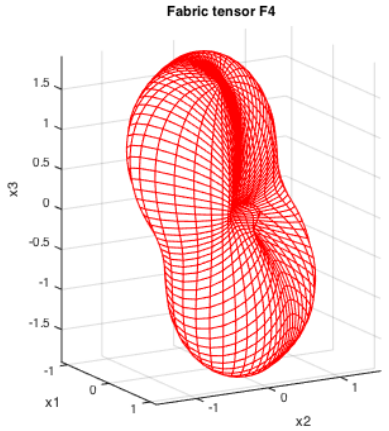

- Use particle size distribution, principal orientation, characteristic shape, fabric tensors, coordination number, to develop a microstructure model
- Use continuum models for porous and granular materials modified by microstructure tensor **F**
- Determine material parameters from experiments
- Approach can be extended to other transport phenomena

Technical Accomplishment: Fabric Tensors

- Fabric tensor of the first kind (moment tensor)

$$N^{(0)} = \frac{1}{N}\sum_{\alpha=1}^{N} 1 = 1 \qquad N_{ij}^{(2)} = \frac{1}{N}\sum_{\alpha=1}^{N} n_i n_j \qquad N_{ijkl}^{(4)} = \frac{1}{N}\sum_{\alpha=1}^{N} n_i n_j n_k n_l$$

- Fabric tensor of the second kind (fabric tensor, least squares based)

$$F^{(0)} = N^{(0)} = 1 \qquad F_{ij}^{(2)} = \frac{15}{2}\left(N_{ij}^{(2)} - \frac{1}{5}\delta_{ij}\right) \qquad F_{ijkl}^{(4)} = \frac{315}{8}\left(N_{ij}^{(4)} - \frac{2}{3}\delta_{ij}N_{kl}^{(2)} + \frac{1}{21}\delta_{ij}\delta_{kl}\right)$$

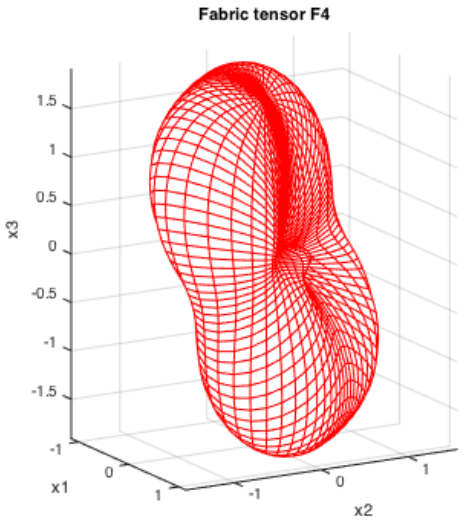

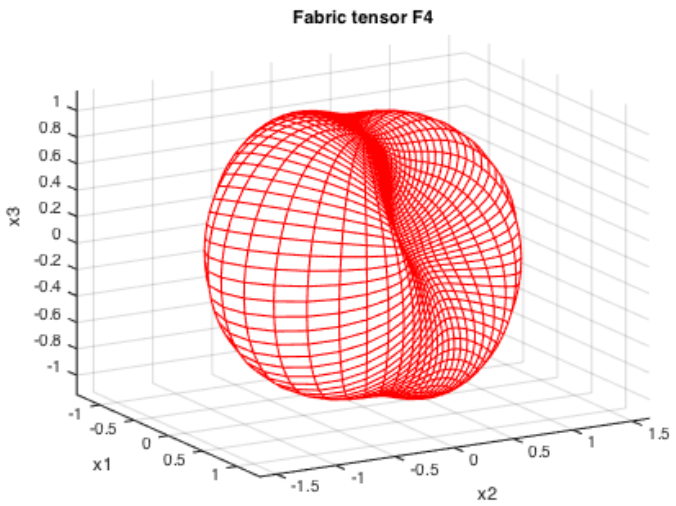

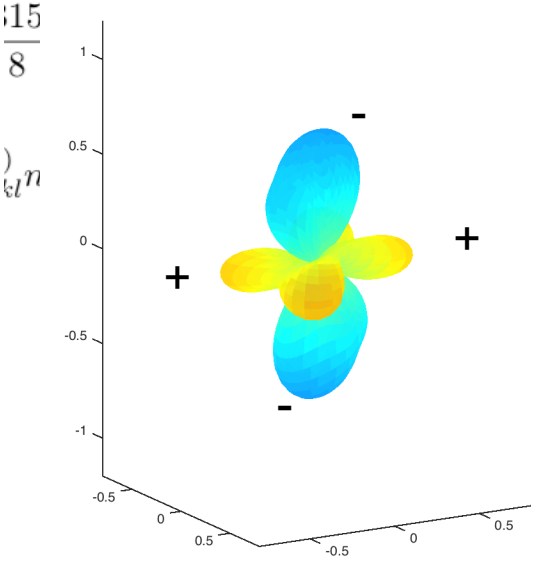

0 bar | 2000 bar | 2000 bar – 0 bar

Key: Yellow-red : positive | Green-blue : negative

OAK RIDGE National Laboratory

Technical Accomplishment : Effect of Calendaring and Composition on Elastic Modulus

90%

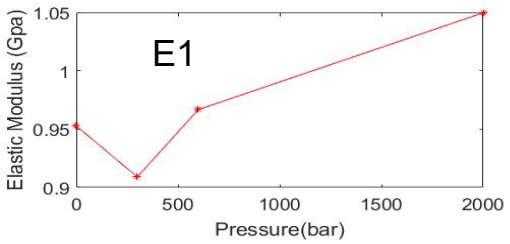

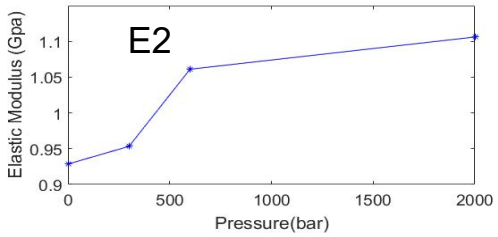

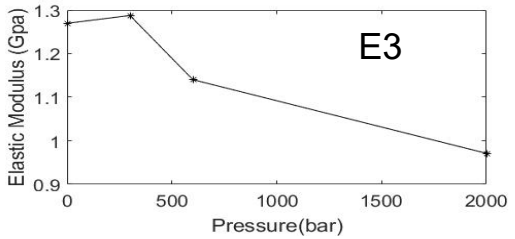

92%

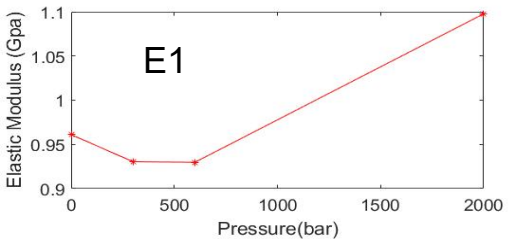

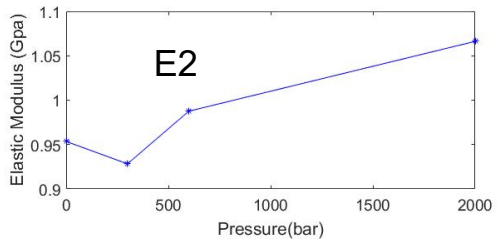

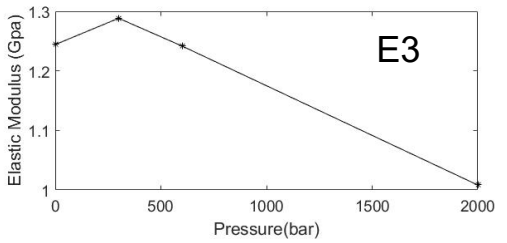

96%

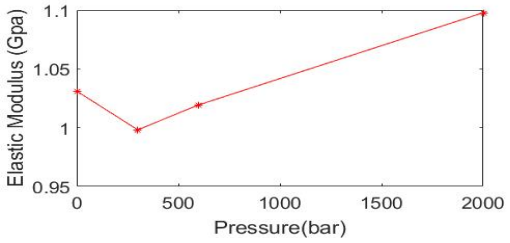

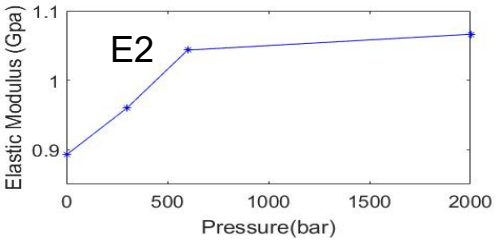

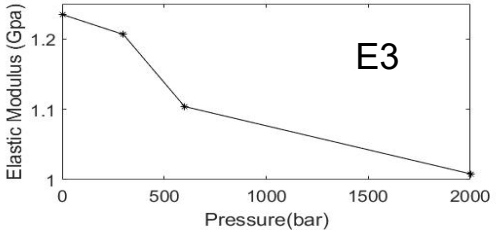

- E1, E2 and E3 are moduli in 3 different directions.
- For isotropic case E1=E2=E3 = 0.82 GPa
- Varying mass fraction of NMC.
- K and G of particles are assumed constant.
- Must be validated with experimental results.

OAK RIDGE National Laboratory

Microstructure-Based Continuum Pressure-Dependent Plasticity Model

- Microstructure is introduced by modifying stress and stiffness tensors by microstructure tensors **F**.

$$J_2 = \frac{1}{6}\left[(\sigma_1 - \sigma_2)^2 + (\sigma_1 - \sigma_3)^2 + (\sigma_2 - \sigma_3)^2\right]$$
$$I_1 = [\sigma_1 + \sigma_2 + \sigma_3]$$
$$\overline{\sigma_{ij}} = \frac{1}{6}\left[\sigma_{ik}F_{kj}^{-1} + F_{ik}^{-1}\sigma_{kj}\right]$$ Modified stress tensor

- The plasticity constitutive model for active material is selected from the family of porous and bonded aggregate materials.

$$\bar{f} = \sqrt{\bar{J}_2^e} - \bar{\alpha}\bar{I}_1^e - \bar{\kappa}$$ Drucker-Prager yield function

- Hat symbols denote microstructure influenced values.
- Material parameters are derived by repeated loading under different combination of confinement and loading.

Technical Accomplishment:
Yield Surface Modification using Fabric Tensor

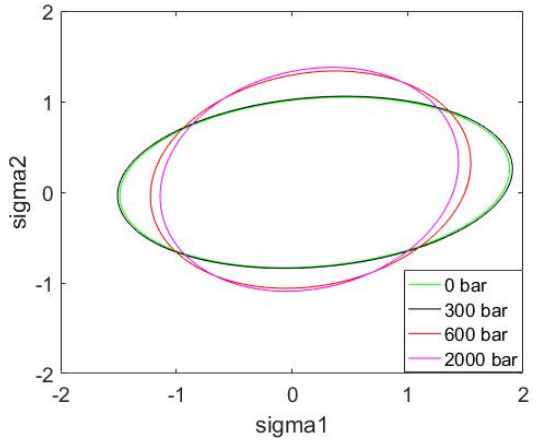

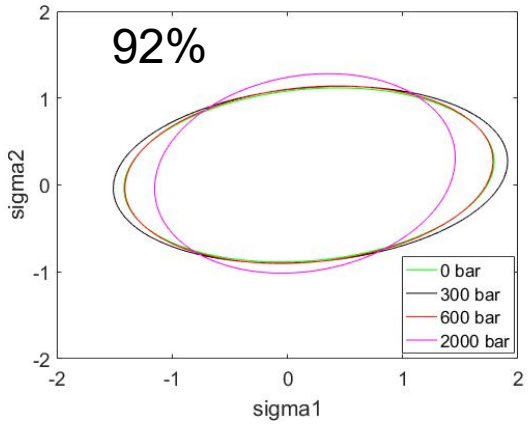

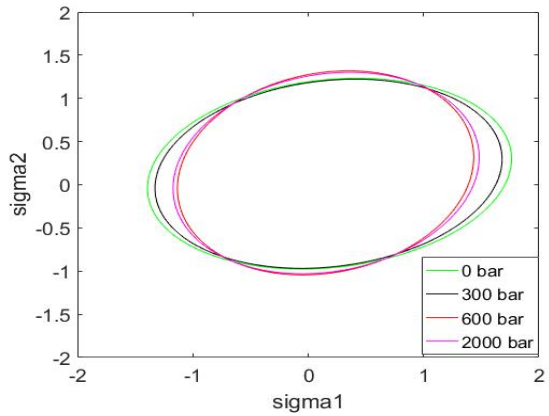

The shape of yield surface changes due to both mass fraction of NMC and calendaring pressure.

Comparison between isotropic yield surface and Fabric Tensor anisotropy for 92% composition

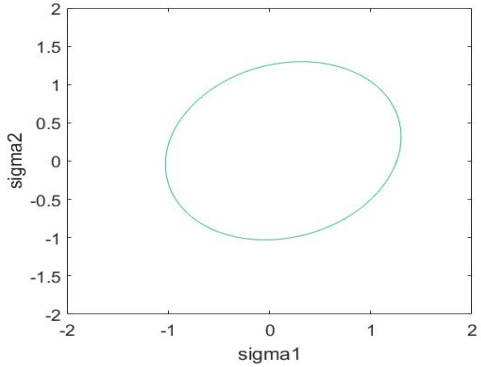

Isotropic

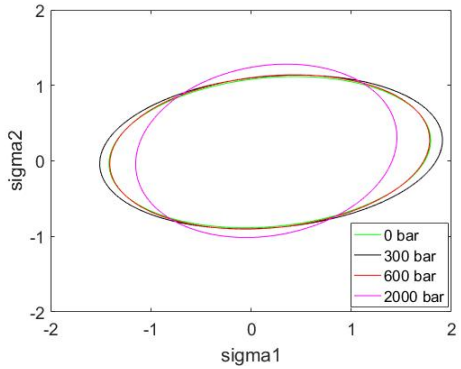

Fabric Tensor

In the isotropic case, yield surface is the same for all the cases as material constants in yield function are assumed to be independent of pressure and NMC mass fraction

OAK RIDGE National Laboratory

Approach : Battery Life Cycle

- For a lithium-ion battery, the life cycle begins with the initial manufacturing/assembling until the end of battery life
- The current study will focus on the repeated charge cycles
  - The rest periods in dashed are optional

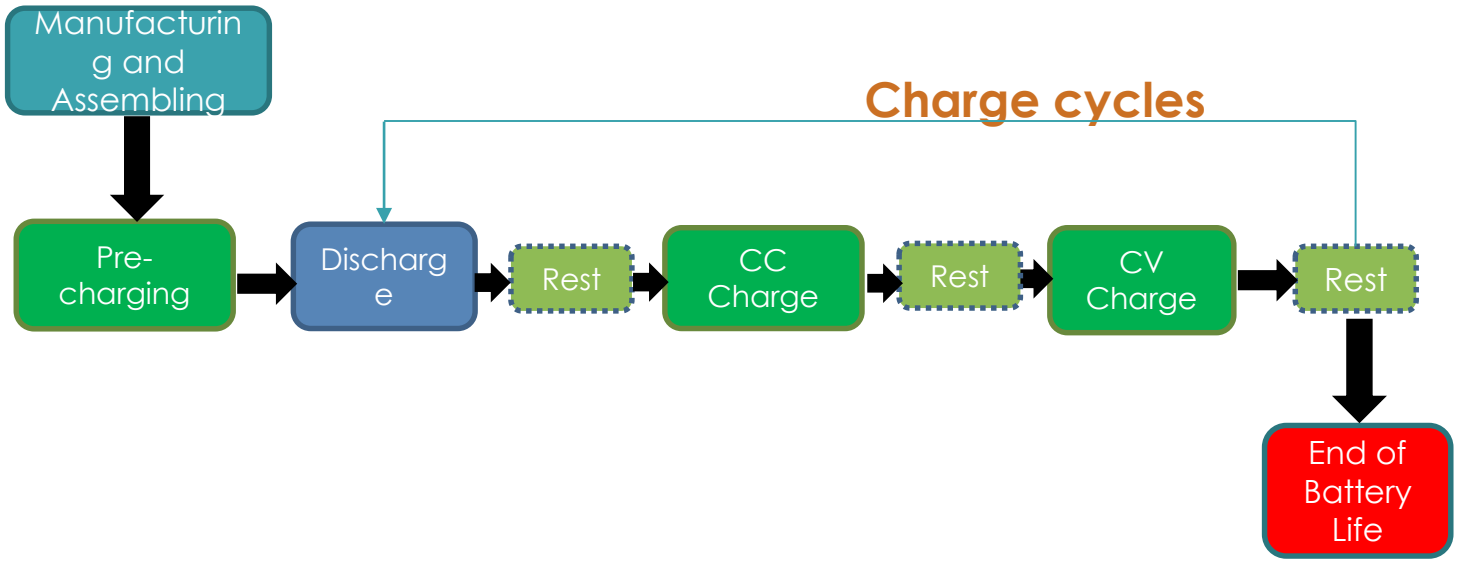

Technical Accomplishment : Validation of full cell simulations NMC 532/A12

Symbol	Units	Anode (A12)	Separator	Cathode (NMC 532)
L		70	25	74
ε_s	-	0.471	-	0.518
ε_e	-	0.503	0.724	0.409
ε_f	-	0.026	-	0.073
c_s^{max}		26390	-	48230
c_s^0		14870	-	3900
c_e^0		2000		
D_s		7.5e-7 cm2/s	-	
D_e		1.0e-9cm2/s		
i_0		1.1	-	0.8
α_a	-	0.5	-	0.5
α_c	-	0.5	-	0.5
t_0^+	-	0.363		
σ		100	-	3.8
R_s		12.5	-	8.5

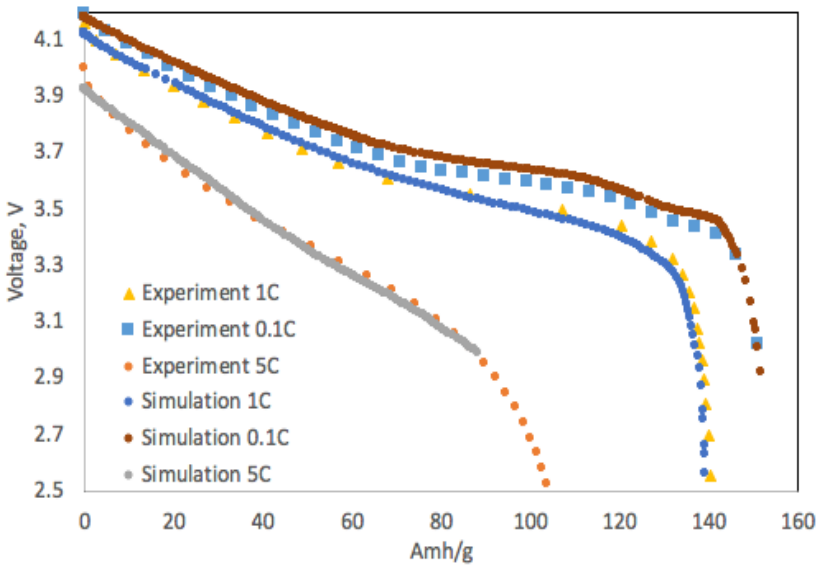

Technical Accomplishment : Charge Protocol - CC and CV

- Higher C rate charging (fast charging) achieves lower capacity
  - Requires longer period of CV charge if charging back to full capacity is needed
- Many factors impact the performance of high C rates
  - Electrode thickness
  - Material properties

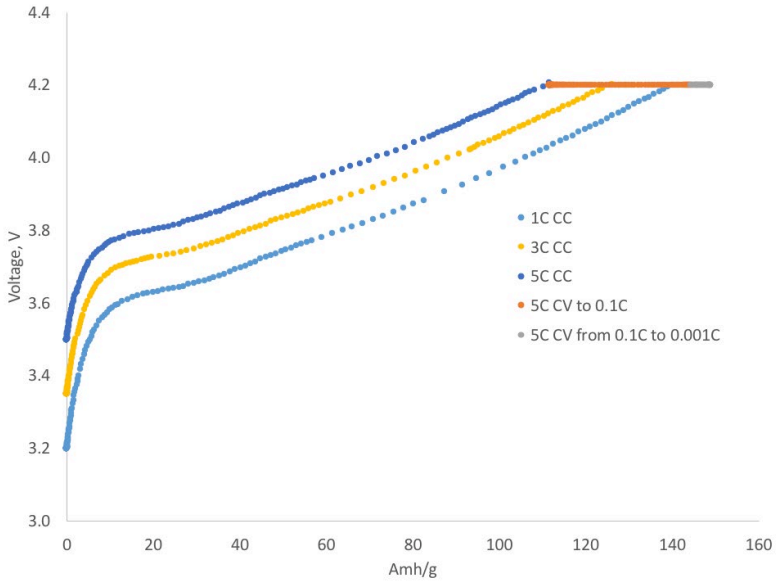

Rate\capacity	Discharge	CC (to V=4.2)	CV (0.1C termination current)	CV (0.001C)
0.1C	150.78	148.29 (99.36%)	NA	149.25 (100%)
1C	150.61	140.14 (93.63%)	146.99 (98.20%)	149.17 (100%)
3C	149.05	126.26 (83.47%)	145.62 (96.27%)	151.26 (100%)
5C	147.70	111.69 (75.21%)	144.45 (97.28%)	148.88 (100%)

Technical Accomplishment: Lithium-ion Concentration in Charge Cycle

Electrolyte

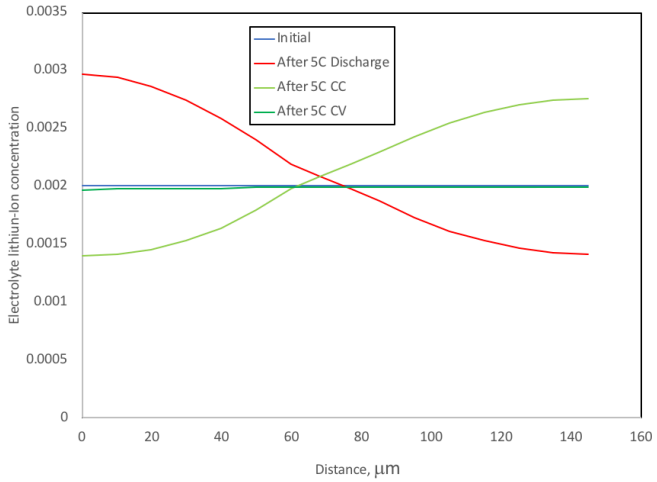

Electrode

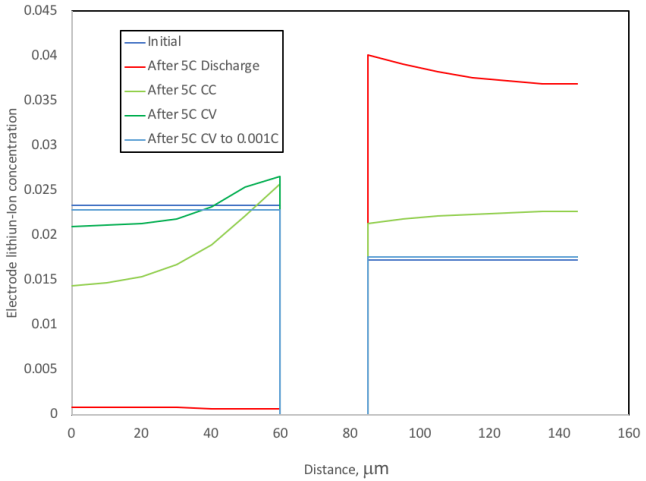

3D Distribution After CC Charge

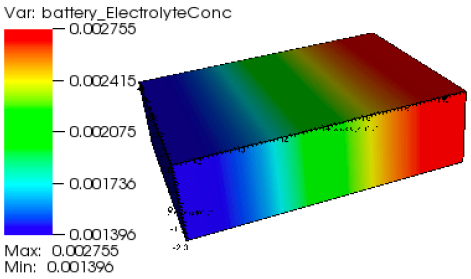

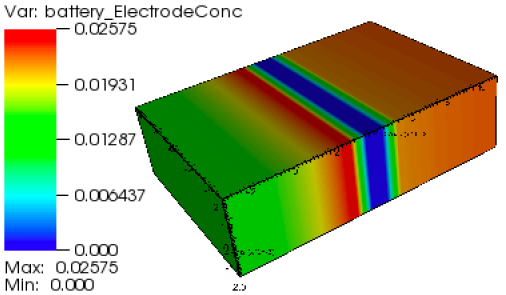

OAK RIDGE National Laboratory

Technical Accomplishment Charge Protocol: CC and CV

- CC of Various C rates
  - Higher C rate yields higher slope
  - Higher resistance (e.g., low transference number) could cause steeper slope and once it reaches 0 ends the charge abruptly
- CV charge
  - Fill the capacity while smoothing the distributions

Electrode

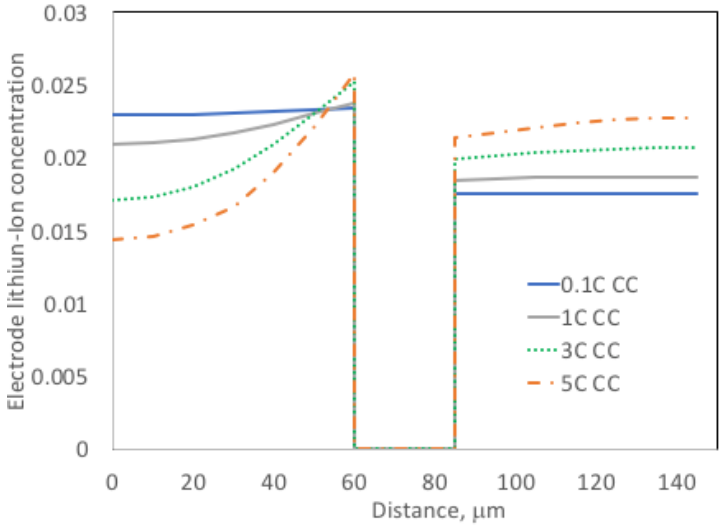

Electrolyte

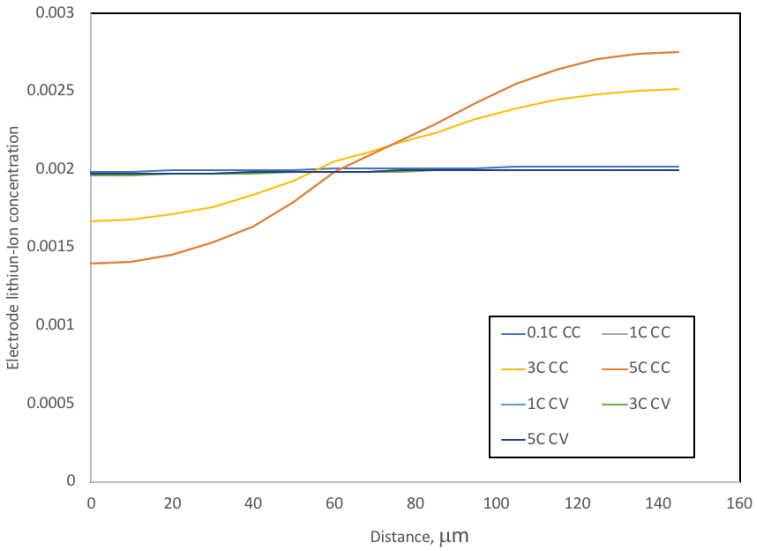

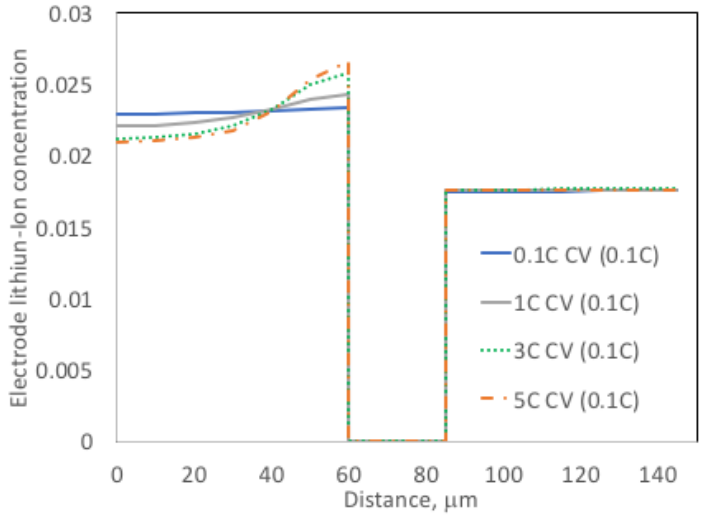

OAK RIDGE National Laboratory

Technical Accomplishment : Condition for Plating During Charge

- During charge, over potential values on anode decreases, and has its minimum value near the separator
- As charge progresses, for higher C rate, over potential will reaches 0 near the separator – a critical condition that lithium plating start to take place

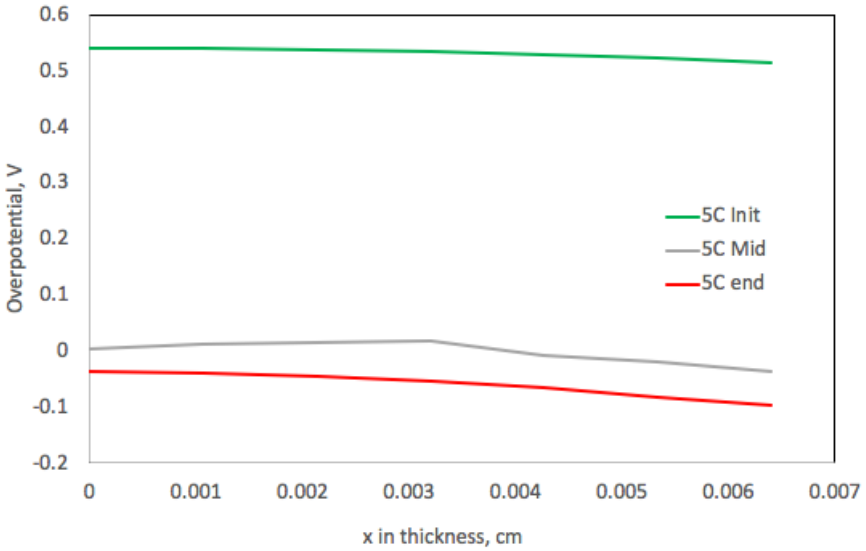

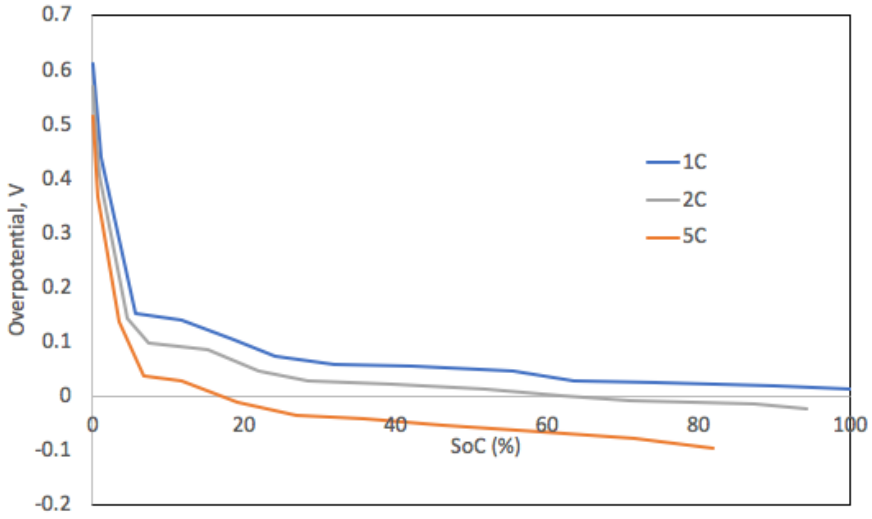

OAK RIDGE National Laboratory

Summary and Remaining Challenges

- We developed a framework for mechanics of battery active materials based on particle assembly formation, non-local microstructural characterization and upscaling to continuum model.
- Initial assessment on plating conditions under various charge protocols is conducted
- Need to introduce inhomogeneities of processed electrodes to model defects or degradation, and see how it impacts the lithium-ion transport and distribution in charge cycle
- Understand the thermal influence on fast charging and plating conditions
- New software release planned for the end of FY19 to be hosted on cloud services at (vibe.ornl.gov) ORNL facility

Publications and Presentations

Peer reviewed journal publications since last AMR (FY17/18):

- Kalnaus, S., Wang, Y., Li, J., Kumar, A., Turner, J.A., Temperature and strain rate dependent behavior of polymer separator for Li-ion batteries, *Extreme Mechanics Letters*, 20C (2018), pp. 73-80.
- Wang, H., Watkins, T.R., Simunovic, S., Bingham, P.R., Allu, S., Turner, J.A., Fragmentation of copper current collectors in Li-ion batteries during spherical indentation, *J. Power Sources* 364 (2017), 432-436.
- Kalnaus, S., Kumar, A., Wang, Y., Li, J., Simunovic, S., Turner, J., Gorney, P., Strain distribution and failure mode of polymer separators for Li-ion batteries under biaxial loading, *J. Power Sources* 378 (2018), 139-145.
- Kalnaus, S. , Wang, Y., Turner, J.A., Mechanical behavior and failure mechanisms of Li-ion battery separators, *J. Power Sources* 348 (2017) 255-263.

Conference presentations

- Allu, S., Elwasif, W., Gorti, S., Kalnaus, S., Kumar, A., Li, J., Sheng, Y., Simunovic, S., Turcksin, B., Turner, J.A., Wang, H., Wang, Y., "Towards understanding mechanical abuse and failure of batteries," 2017 AABC Conference, June 19 2017, San Francisco, CA.